Continuous and discontinuous radiofrequency energy delivery on the atrial free wall: Lesion transmurality, width, and biophysical characteristics

Daniel J. Friedman, MD,* Jed A. Overmann, DVM, MS, DACVP,† Jeffrey M. Fish, DVM,† Stephen A. Gaeta, MD, PhD,‡ John H. Tranter, MSEE,† Riki Thao, AOT,† Jonathan P. Piccini, MD, MHS, FHRS*

*From the *Electrophysiology Section, Duke University Hospital, Durham, North Carolina, †Abbott, St. Paul, Minnesota, and ‡Inova Heart and Vascular, Falls Church, Virginia.*

BACKGROUND Although lesion transmurality is required for durable pulmonary vein isolation, excess ablation is associated with increased risk of complications.

OBJECTIVE We sought to understand the impact of interrupted radiofrequency (RF) delivery conditions on lesion characteristics in the atrial free wall.

METHODS Thirty-three (11 left atrial, 22 right atrial) RF ablation lesions were created in the atria of 6 swine using power control mode (25 W, target contact force 15 g) with 1 of 3 conditions: 15 seconds ablation (n = 8), 30 seconds ablation (n = 14), or 2 15-second ablations at the same site separated by a 2-minute interruption (15 seconds × 2) (n = 11).

RESULTS Thirty of 33 lesions were transmural. Rates of transmurality ($P = .45$) and endocardial lesion width (5.6 ± 1.2 mm, $P = .70$) were similar between conditions. Mean tissue thickness was 1.7 ± 0.8 mm for transmural lesions. Wide variability in bipolar electrogram attenuation was observed across and within conditions and there were no significant between-group differences. Although impedance reductions were numerically greater in the 30-second and 15-second × 2 conditions (-14.6 ± 6.6 ohms and -14.0 ± 4.4 ohms, respectively) compared to the 15-second condition (-10.3 ± 6.4 ohms), variability was large, and differences were not statistically significant ($P = .243$). Impedance changes after ablation were largely transient.

CONCLUSION A single 15-second ablation at 25 W (target contact force of 15 g) with good stability produced similarly sized lesions compared to 30-second ablations and 2 15-second ablations at the same site in atrial free wall tissue. These data suggest over-ablation in the atria is common, larger-diameter lesions may require greater power, and many clinically available parameters of lesion size may be unreliable on the posterior wall.

KEYWORDS Ablation; Atrial fibrillation; Catheter ablation; Lesion formation; Radiofrequency; Radiofrequency ablation

(Heart Rhythm O2 2021;2:635–641) Published by Elsevier Inc. on behalf of Heart Rhythm Society.

Introduction

The success of pulmonary vein isolation is dependent on the generation of transmural and contiguous ablation lesions. The free walls (including the posterior wall) are typically the thinnest portion of the left atrium.[1] While this makes lesion transmurality more achievable, it also increases the risk of complications related to excess energy delivery, including pericarditis, vagal injury (gastric and esophageal hypomotility),[2] atrioesophageal fistula,[3] and perforation. Owing to increasing interest in posterior wall isolation as a strategy for reducing recurrent atrial fibrillation (AF) in the setting of nonparoxysmal AF,[4–6] optimal energy titration is essential for maximizing safety and efficacy. A recent publication[7] has emphasized the overall poor rates of durable posterior wall isolation and underscored the need to better understand ablation of this important aspect of the left atrium.

Although numerous studies have evaluated posterior wall ablation during clinically indicated ablations in humans, these studies are limited by the inability to assess individual lesion transmurality. To meet the clinical need for more data regarding optimal radiofrequency (RF) energy delivery on the left atrial free wall, we performed a series of in vivo porcine experiments where individual RF lesions were delivered to several sites within the atrial free wall using different experimental conditions.

Methods

The protocol for this study was approved by the Institutional Animal Care and Use Committee (IACUC) and conforms to the Guide for the Care and Use of Laboratory Animals. Six

Address reprint requests and correspondence: Dr Daniel J. Friedman, Section of Cardiac Electrophysiology, Duke University Hospital, 2301 Erwin Rd, Durham, NC 27710. E-mail address: daniel.friedman@duke.edu.

2666-5018/Published by Elsevier Inc. on behalf of Heart Rhythm Society.

https://doi.org/10.1016/j.hroo.2021.10.012

KEY FINDINGS

- With radiofrequency ablation on the atrial free wall using 25 W and 15 g of contact force, lesion diameter (5.5–6.0 mm) and transmurality (91%) were similar with a 15-second, 30-second, or 2 separate 15-second ablation applications; this suggests over-ablation is common on the atrial free wall.
- Substantial variability in bipolar electrogram changes were observed with ablation such that it did not seem to correlate with energy delivery via either of the 3 above conditions.
- Although unipolar tip impedance change with ablation is commonly monitored as a proxy for lesion formation, we observed that after cessation of ablation the impedance typically returns to a value close to the preablation baseline.

male Yorkshire cross swine (49–66 kg, 3 months) were premedicated with oral amiodarone (600 mg, orally, daily) starting 3 days prior to the procedure. After a 12-hour fast, animals were induced with tiletamine/zolazepam and xylazine (3.5–5.5 mg/kg each, intramuscularly) and general anesthesia was maintained with isoflurane inhalation (1%–1.75%). Heart rate, body temperature, mean blood pressure, oxygen saturation, electrocardiogram tracing, end-tidal CO_2, respiratory rate, inspiratory pressure, and tidal volume were monitored throughout the procedure to assess ventilation and hemodynamic state. Animals were placed in a supine position and percutaneous femoral arterial and venous access and jugular venous access were obtained. A decapolar catheter was placed in the coronary sinus (Response™ CSL™; Abbott, St. Paul, MN) and transseptal access was obtained. Activated clotting times were maintained >300 seconds throughout the procedure by administration of heparin. Atrial geometries were obtained using the EnSite Precision™ cardiac mapping system (Version 2.2; Abbott, St. Paul, MN) and the Advisor™ HD Grid Mapping Catheter, Sensor Enabled™ (Abbott, St. Paul, MN). Ablation lesions were created in the right and left atria using a 3.5 mm open irrigated ablation catheter (TactiCath™ Contact Force Ablation Catheter, Sensor Enabled™; Abbott, St. Paul, MN) connected to an RF ablation generator (Ampere™ RF Ablation Generator; Abbott, St. Paul, MN). A single grounding pad (Valleylab E7506; Medtronic, Minneapolis, MN) was applied on the mid back. During ablations, the catheter was irrigated at 17 mL/min with heparinized (1000 U/L) 0.9% saline using a Cool Point™ Irrigation Pump (Abbott, St. Paul, MN). In addition, the catheter was connected to TactiSys™ Quartz hardware (Abbott, St. Paul, MN) to monitor catheter tip contact force.

Atrial ablations were created with a power of 25 W in power-controlled mode with 1 of 3 conditions: a single 15-second ablation (15s), a single 30-second ablation (30s), or 2 15-second ablations (15s × 2) at the same location separated by a 2-minute pause in energy delivery. Targeted contact force for all conditions was 15 g. Ablation conditions were blocked by chamber and randomized to ensure ablation conditions were being applied in each chamber in a random order and ablation conditions were balanced across chambers. Lesions were targeted on the posterior/posterior-lateral aspect of the right atrium and the posterior wall of the left atrium. Five to 6 lesions were placed in each right atrial chamber, while 3–4 lesions were placed in each left atrial chamber.

Following euthanasia, the heart and lungs were removed. The heart was then perfused with 1% triphenyltetrazolium chloride stain. Following staining, the heart was fixed in 10% buffered formalin for a minimum of 10 days. Tissue dissection and lesion measurements occurred after the completion of the fixation period. Maximum gross lesion width on the endocardial surface was measured with a digital caliper (Mitutoyo Absolute AOS Digimatic; Mitutoya Corporation, Kawasaki, Japan). Lesions were then transected to assess for transmurality.

Electrograms were exported from the EnSite Precision mapping system and analyzed using Matlab (Mathworks, Natick, MA). The mean peak-to-peak bipolar voltage was compared between the 3 beats preceding the start of ablation and the 3 beats immediately following the end of ablation. Electrogram reductions for the 15s × 2 condition were determined as baseline at the beginning of the first ablation minus the value after the second ablation. Other parameters determined for the 3 ablation conditions were mean force (g), impedance change (Ω), force-time integral (FTI) (g·s), and mean current (milliamperes). For the 15s × 2 condition, mean values were determined by the mean of the 2 ablations. For FTI the values for the 15s × 2 condition were determined as the summed value of the 2 ablations. Impedance change for the 15s × 2 condition was determined as the impedance at the end of the second ablation minus the impedance at the beginning of the first ablation.

Statistical tests that were performed included the Shapiro-Wilk test for normality, Brown-Forsythe test for equal variance, 1-way ANOVA with Holm-Sidak method for pairwise comparison (for data passing both normality and equal variance), Kruskal-Wallis 1-way ANOVA (for data failing normality and/or equal variance tests), 2 × 3 Fisher test, and paired *t* test. Statistical analysis of data was performed using Minitab 17.1.0 (Minitab Inc, State College, PA) and SigmaPlot 13.0 (Systat Sofware, Inc, San Jose, CA). A *P* value of .05 was used to denote significance. The data underlying this article will be shared on reasonable request to the corresponding author.

Results

Lesion characteristics

A total of 52 RF lesions were delivered across 6 animals and 33 lesions (11 left atrial, 22 right atrial) were in free wall locations and were acceptable for analysis. No steam pops occurred. The mean time between ablation and euthanasia

Table 1 Lesion size, contact force, lesion size surrogate measures, and lesion transmurality by ablation condition

	Ablation condition			
	15s (N = 8)	15s × 2 (N = 11)	30s (N = 14)	*P* value
Lesion size				
Lesion width (mm)[†,‡]	5.9 ± 1.0 A	5.5 ± 0.8 A	5.6 ± 1.5 A	.704
Contact force				
Mean contact force (g)[†,‡,§]	15.7 ± 3.5 A	15.5 ± 3.2 A	15.3 ± 3.1 A	.965
Predictors of lesion size				
Impedance change (Ω)[†,‡,‖]	-10.3 ± 6.4 A	-14.0 ± 4.4 A	-14.6 ± 6.6 A	.243
% Reduction in impedance (Ω)[†,‡,¶]	10.0 ± 6.0 A	13.6 ± 3.9 A	13.5 ± 5.4 A	.248
Force time integral (g•s)[†,‡,#]	233 ± 52 A	462 ± 96 B	457 ± 93 B	<.001
Mean current (milliamperes)[†,‡,§]	513.0 ± 37.4 A	517.8 ± 29.2 A	521.1 ± 34.2 A	.861
Reduction in peak to peak bipolar voltage (mV)[†,**,††]	0.378 (1.178) A	1.575 (1.432) A	1.290 (1.225) A	.154
% Reduction in peak to peak bipolar voltage[†,**,‡‡]	53.6 (53.5) A	68.7 (38.6) A	64.7 (25.2) A	.243
Transmurality				
% Transmural lesions[†,§§]	88% A	100% A	86% A	.450

Ablation conditions are as follows: a single 15-second ablation (15s), 2 15-second ablations (15s × 2), and a single 30-second ablation (30s).

[†]Values that do not share a letter are significantly different.

[‡]One-way ANOVA, $\alpha = 0.05$ with Holm-Sidak method for pairwise comparison.

[§]Value for 15s × 2 is the average of the 2 ablations.

[‖]Value for 15s × 2 is impedance at end of second ablation minus impedance at beginning of first ablation.

[¶]Value for 15s × 2 is $\frac{\text{start of 1st ablation} - \text{end of 2nd ablation}}{\text{start of 1st ablation}} * 100\%$.

[#]Force-time integral for 15s × 2 is the summed value.

**Kruskal-Wallis 1-way ANOVA on ranks, $\alpha = 0.05$.

[††]Electrogram reduction for 15s × 2 is baseline at the beginning of first ablation minus value after second ablation.

[‡‡]Value for 15s × 2 is $\frac{\text{mV baseline of 1st ablation} - \text{mV after 2nd ablation}}{\text{mV baseline of 1st ablation}} * 100\%$.

[§§]2 × 3 Fisher test.

was 108 ± 27 minutes. Lesions were excluded owing to the following: septal location (n = 4), location within trabeculation (n = 4), overlapping lesions (n = 2), inability to identify lesions during necropsy (n = 3), catheter instability (n = 2), inadvertent damage to lesions during necropsy (n = 2), atypical appearance (n = 1), and location within a pulmonary vein ostium (n = 1). Mean contact force did not significantly differ by treatment group (15s: 15.7 ± 3.5 g, 15s × 2: 15.5 ± 3.2 g, 30s: 15.3 ± 3.1 g, $P = .965$). Although the mean power delivery was slightly higher in the 30s group (24.4 ± 0.006 W) compared to the other conditions (15s: 23.9 ± 0.008 W and 15s × 2: 23.9 ± 0.002 W, $P < .001$) owing to the 2-second power ramp-up, the mean current delivery was similar across ablation conditions ($P = .861$). Characteristics of all analyzable lesions are detailed in Table 1. Representative lesions for each ablation condition are depicted in Figure 1.

Lesion transmurality

Lesion transmurality was very common and did not vary based on treatment group (15s: 88%, 15s × 2: 100%, 30s: 86%, $P = .450$; Figure 2). Mean tissue thickness was 1.7 ± 0.8 mm for transmural lesions. Maximum lesion width was consistent across treatment groups (15s: 5.9 ± 1.0 mm, 15s × 2: 5.5 ± 0.8 mm, 30s: 5.6 ± 1.5 mm, $P = .704$). There were no qualitative differences in lesion morphology by experimental condition. The 2 nontransmural 30-second lesions and 1 nontransmural 15-second lesion were at the base of the left atrial appendage in relatively thicker tissue, which is also adjacent to the left azygos vein.

The relationship between lesion condition, transmurality, and a variety of lesion parameters is depicted in a series of individual value plots (Figure 3). Although impedance reductions were slightly lower among nontransmural lesions, reductions were overall similar to those observed with numerous transmural lesions. It is notable that the 2 nontransmural 30-second lesions had greater mean current delivery compared to the 30-second transmural lesions.

Biophysical parameters of repeat ablation at the same location

The mean contact force of the first 15-second lesion was less than the second 15-second lesion (14.7 ± 3.1 g vs 16.2 g, $P =$

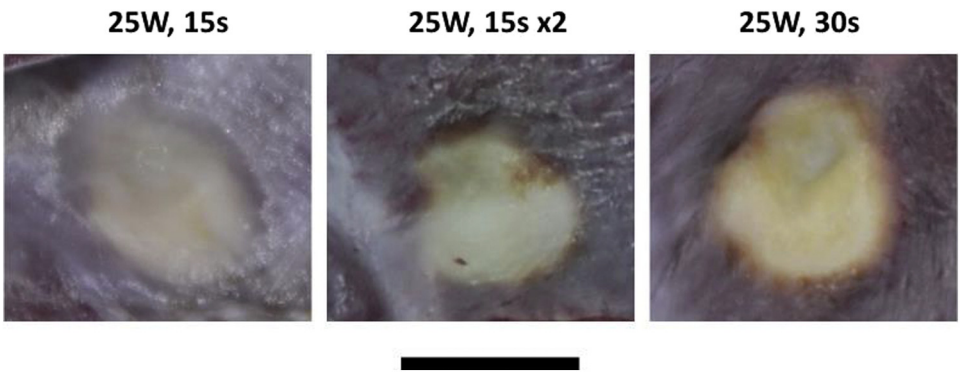

Figure 1 Representative gross pathology specimens. Black bar represents 5 mm.

.012), resulting in a slightly smaller FTI associated with the first 15-second lesion (vs 220 ± 46 g•s vs 242 ± 53 g•s, $P = .015$). The absolute and relative impedance changes were no different among the first or second 15-second lesion ($P = .521$ and $P = .385$, respectively). The mean current was slightly less with the first 15-second lesion (512.9 ± 29.1 mA vs 522.7 ± 29.4 mA, $P < .001$). The absolute and relative bipolar electrogram amplitude reductions were greater with the first vs second 15-second lesion (1.592 ± 1.069 mV vs 0.043 ± 0.139 mV, $P < .001$, and 67.1% ± 27.4% vs 5.0% ± 2%, $P < .001$).

Several trends in unipolar impedance were observed with the 15s × 2 condition. Impedance reduction during the first RF application was -11.0 ± 4.7 ohms compared to -11.7 ± 3.5 ohms during the second application ($P = .521$). The qualitative characteristics of the impedance curves corresponding to the first and second 15-second application were overall similar (Figure 4). There was a small and statistically significant difference in the tissue impedance at the beginning of the first RF application compared to the beginning of the second RF application (102.5 ± 8.2 ohms vs 100.1 ± 8.3 ohms, $P = .002$), although the magnitude of difference was small (2.4 ohms).

Discussion

The report, which examined the impact of different ablation conditions on lesion characteristics on the porcine atrial free wall, has several clinically relevant findings. First, with ablation employing 15 g of force, 25 W in a power-controlled mode, and good catheter stability, ablation beyond 15 seconds did not measurably increase the rate of transmurality. Substantial variability in bipolar electrogram changes were observed with ablation such that it did not appear to correlate with energy delivery. Although impedance reductions were numerically greater in the 30s and 15s × 2 conditions compared to the 15s condition, variability was large, and differences were not statistically significant. Unipolar tip impedance decreased with each RF application but typically returned close to preablation values after RF application concluded. Lesion width was 5.5–6 mm and generally did not increase with either a second 15-second RF application or a total of 30 seconds.

We observed that with 25 W ablation in power-controlled mode with 15 g of contact force, lesions were frequently transmural and were of approximately 5.5–6.0 mm in diameter. Somewhat surprisingly, increased duration of ablation, with either a total of 30 consecutive seconds of

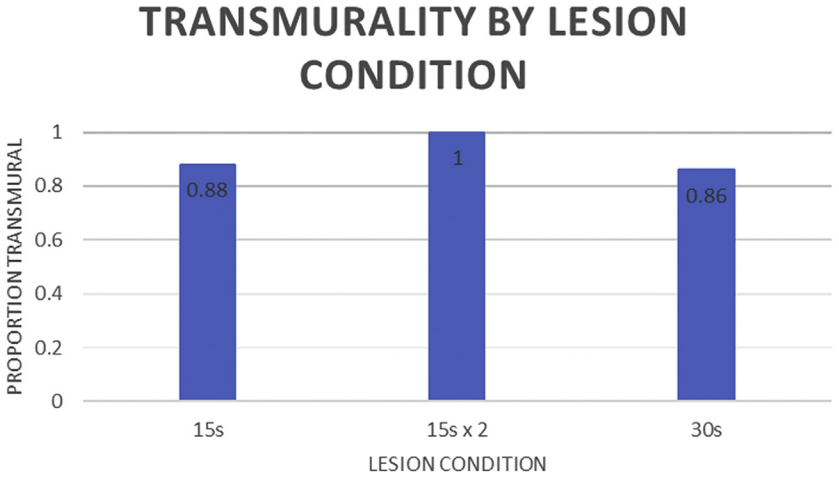

Figure 2 Proportion of transmural lesions by ablation condition. There was no significant difference in transmurality by condition ($P = .450$).

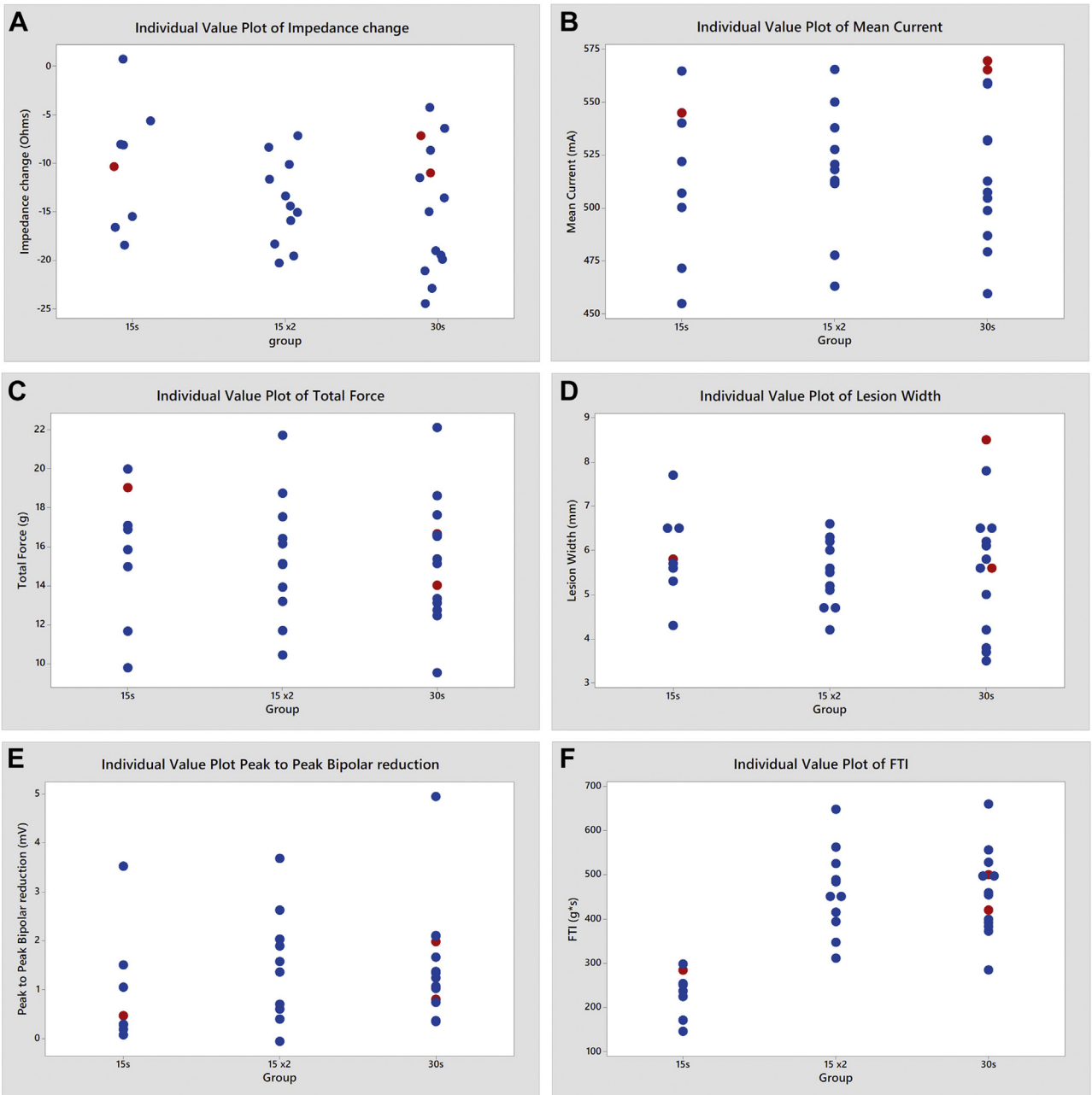

Figure 3 Individual value plots depicting lesion parameters including transmurality (blue circles indicate transmural, red circles indicate nontransmural) by ablation condition (a single 15-second ablation [15s], 2 15-second ablations [15s × 2], and a single 30-second ablation [30s]). Reported lesion parameters include impedance change (**A**), mean current (**B**), mean force (**C**), lesion width (**D**), bipolar electrogram reduction (**E**), and force time integral (FTI) (**F**).

ablation or a second 15-second RF application, did not increase the lesion diameter. A previously published study on RF energy titration using an ex vivo model demonstrated that increasing either power or ablation duration could increase lesion depth and diameter.[8] However, the impact of increasing ablation *duration* was less compared to the impact of increasing ablation *power*. Furthermore, the impact of increasing ablation duration was *less* at lower powers. The results from a prior in vivo study demonstrated that although increasing duration of ablation with either longer duration of ablation or a second RF application has the potential to increase lesion depth,[9] the current study demonstrates it is typically not necessary on the thin atrial free wall and could therefore increase collateral damage during ablation. The results from our study additionally demonstrate that if wider ablation lesions are desired, higher power may be necessary. However, this could be at the cost of more collateral damage if ablation duration is not sufficiently limited.

Peak-to-peak bipolar electrogram amplitude decreased at least somewhat during all RF applications but was not tightly correlated with RF condition. Our results are different from

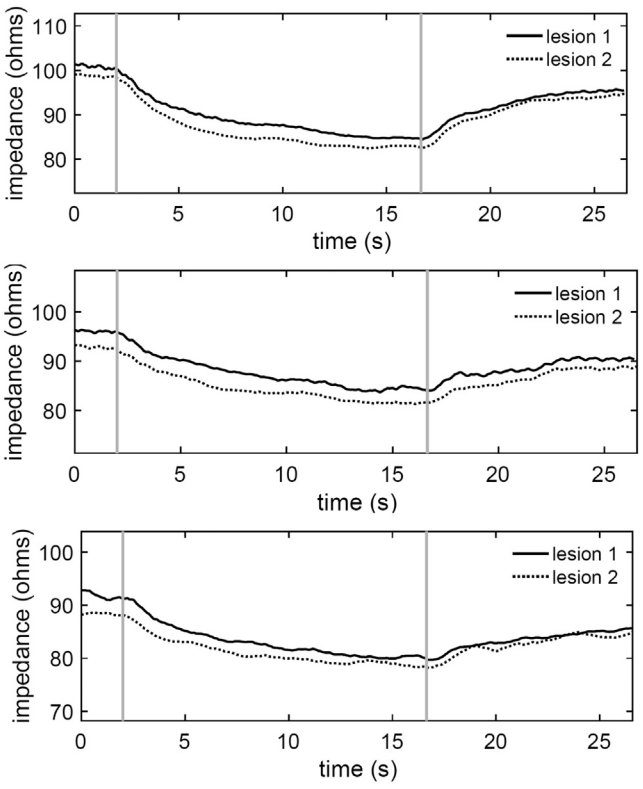

Figure 4 Three examples of the impedance trends observed with repeat radiofrequency (RF) application at the same site. Superimposition of impedance curves for the first (*solid line*) and second (*dotted line*) RF applications reveals both are qualitatively similar.

some previous studies that have identified a good correlation between RF delivery and electrogram attenuation.[10–14] We hypothesize that at least part of the paradoxical findings relates to the relatively large antennae of a 3.5-mm-tip electrode relative to overall thin atrial tissue (∼2 mm) resulting in an unfavorable signal-to-noise ratio. However, we note that a 2 mm wall thickness is common on the human left atrial posterior wall and roof.[1]

The 15s × 2 ablation lesion condition allowed for a unique assessment of temporal changes during and after RF energy delivery (during the 2-minute waiting period). Although we observed an average >10-ohm impedance drop with a 15-second RF application, the unipolar tissue impedance often returned close to baseline prior to initiation of the second RF application. This suggests that the impedance change with atrial ablation is a better reflection of temporary tissue change (eg, temperature rise during ablation) rather than an indicator of permanent tissue destruction. As such, unipolar tip impedance should not be considered as a method for identifying recently ablated atrial tissue. Similarly, since the magnitude of impedance drop and qualitative characteristics of the impedance curves were similar for initial and repeat RF applications, the response to ablation should not be considered a justification for repeat or ongoing ablation in a region.

Clinical implications

This set of experiments has several findings relevant to clinical atrial ablation of the left atrial free wall. So long as there is not marked atrial hypertrophy and force and stability are satisfactory, no more than 15 seconds should be necessary to achieve transmural ablation on the atrial free wall with 25 W or more. Moreover, our data suggest that ablation beyond 15 seconds does not increase lesion diameter and greater power (beyond the 25 W used in this study) is likely required to achieve larger-diameter lesions. With 25 W of ablation, the average maximum lesion diameter is 5.5–6.0 mm with a standard deviation of ∼1.0 mm. Thus, to ensure contiguous lesions with use of the TactiCath, spacing should be no more than ∼4 mm. If greater lesion diameter is desired, higher power should be used; to avoid the potential for collateral damage to surrounding structures, shorter ablation duration should be considered. The relationship between lesion diameter and FTI observed in this study demonstrates that the clinical utility of this metric (and others) may vary based on the site of ablation. Specifically, in this study, although the FTI of the 15s lesion was ∼50% less than the other 2 conditions (a significant difference), the lesion diameter was the same. Overall, the results of this study underscore that optimal RF ablation in the left atrium requires careful selection of power and clinically available lesion size prediction algorithms. Finally, the proximity between the nontransmural lesions and vascular structure (left azygos vein, which connects to the porcine coronary sinus[15]) underscores that ablation strategy may require modification in close proximity to heat sinks.

Limitations

This study has several important limitations. This study evaluated lesion characteristics in porcine atria, which, although used frequently for lesion formation research, may be different from human atria in important ways (eg, presence of a large left azygos vein).[15] However, we note that the tissue thickness of the ablated regions in the current study are similar to the posterior wall and roof in the human left atria.[1] The atria in this study were normal and, as such, the results may not be generalizable to atria with extensive myopathy or thicker atrial regions, such as the septum and ligament of Marshall. This study used a single power, ablation mode, target contact force, and irrigation rate. As such, the results may have limited generalizability to RF delivery with other parameters. This study utilized TactiCath and the generalizability to other catheter designs is unclear. The unipolar electrograms were not of sufficient quality for analysis. Finally, the number of lesions in this study may limit the power to statistically detect small differences.

Conclusion

In the atrial free wall, 15-second RF lesions using 25 W with 15 g contact force and good stability produced lesions of similar diameters (∼5.5 mm) compared to lesions generated with 1 30-second or 2 15-second RF applications. Lesion transmurality was very common (91%) and similar across

ablation conditions. These data suggest over-ablation in the atrial free walls is common. To achieve larger-diameter lesions, greater power is required. Ablation-induced changes in tissue impedance are mostly transient and likely reflect changes in tissue temperature. Finally, available parameters of lesion size may be unreliable on the posterior wall.

Funding Sources

This work was funded by Abbott.

Disclosures

Dr Friedman has received research support from Boston Scientific, Biosense Webster, and Abbott; educational grants from Boston Scientific, Medtronic, Abbott, and Biotronik; and consulting fees from Abbott. Dr Gaeta has received research support from Boston Scientific and serves as a consultant to Biosense Webster. Dr Piccini receives grants for clinical research from Abbott, American Heart Association, Boston Scientific, Gilead, Janssen Pharmaceuticals, NHLBI, and Philips and serves as a consultant to Abbott, Allergan, ARCA Biopharma, Biotronik, Boston Scientific, Johnson & Johnson, LivaNova, Medtronic, Milestone, Oliver Wyman Health, Sanofi, Philips, and Up-to-Date. Mr Thao, Mr Tranter, and Drs Overmann and Fish are employees of Abbott.

Authorship

All authors attest they meet the current ICMJE criteria for authorship.

Ethics Statement

The protocol for this study was approved by the Institutional Animal Care and Use Committee and conforms to the Guide for the Care and Use of Laboratory Animals.

References

1. Hall B, Jeevanantham V, Simon R, Filippone J, Vorobiof G, Daubert J. Variation in left atrial transmural wall thickness at sites commonly targeted for ablation of atrial fibrillation. J Interv Card Electrophysiol 2006;17:127–132.
2. Oikawa J, Fukaya H, Wada T, et al. Additional posterior wall isolation is associated with gastric hypomotility in catheter ablation of atrial fibrillation. Int J Cardiol 2021;326:103–108.
3. Kapur S, Barbhaiya C, Deneke T, Michaud GF. Esophageal injury and atrioesophageal fistula caused by ablation for atrial fibrillation. Circulation 2017; 136:1247–1255.
4. Bai R, Di Biase L, Mohanty P, et al. Proven isolation of the pulmonary vein antrum with or without left atrial posterior wall isolation in patients with persistent atrial fibrillation. Heart Rhythm 2016;13:132–140.
5. DeLurgio DB, Crossen KJ, Gill J, et al. Hybrid convergent procedure for the treatment of persistent and long-standing persistent atrial fibrillation: results of CONVERGE clinical trial. Circ Arrhythm Electrophysiol 2020;13:e009288.
6. Thiyagarajah A, Kadhim K, Lau DH, et al. Feasibility, safety, and efficacy of posterior wall isolation during atrial fibrillation ablation: a systematic review and meta-analysis. Circ Arrhythm Electrophysiol 2019;12:e007005.
7. Markman TM, Hyman MC, Kumareswaran R, et al. Durability of posterior wall isolation after catheter ablation among patients with recurrent atrial fibrillation. Heart Rhythm 2020;17:1740–1744.
8. Borne RT, Sauer WH, Zipse MM, Zheng L, Tzou W, Nguyen DT. Longer duration versus increasing power during radiofrequency ablation yields different ablation lesion characteristics. JACC Clin Electrophysiol 2018;4:902–908.
9. Friedman DJ, Overmann JA, Fish JM, et al. Impact of interruptions in radiofrequency energy delivery on lesion characteristics. Heart Rhythm 2020; 17:1354–1359.
10. Otomo K, Uno K, Fujiwara H, Isobe M, Iesaka Y. Local unipolar and bipolar electrogram criteria for evaluating the transmurality of atrial ablation lesions at different catheter orientations relative to the endocardial surface. Heart Rhythm 2010;7:1291–1300.
11. Tomlinson DR, Myles M, Stevens KN, Streeter AJ. Transmural unipolar electrogram change occurs within 7 s at the left atrial posterior wall during pulmonary vein isolation. Pacing Clin Electrophysiol 2019;42:922–929.
12. Coeman M, Haddad ME, Wol M, et al. 'CLOSE'-guided pulmonary vein isolation and changes in local bipolar and unipolar atrial electrograms: observations from the EP lab. J Atr Fibrillation 2018;10:1794.
13. Kogawa R, Watanabe I, Okumura Y, et al. Usefulness of filtered unipolar electrogram morphology for evaluating transmurality of ablated lesions during pulmonary vein isolation. J Arrhythm 2016;32:108–111.
14. Michowitz Y, Buch E, Bourke T, et al. Unipolar and bipolar electrogram characteristics predict exit block during pulmonary vein antral isolation. Pacing Clin Electrophysiol 2012;35:1294–1301.
15. Crick SJ, Sheppard MN, Ho SY, Gebstein L, Anderson RH. Anatomy of the pig heart: comparisons with normal human cardiac structure. J Anat 1998; 193:105–119.